N-63-4-3

CATALOGED BY DDC
AS AD No. 410116

SOLID ROCKET PLANT

ACOUSTICAL ANALYSIS OF FILAMENT-WOUND
POLARIS CHAMBERS

Contract NOw 62-1007c (FBM)

Bimonthly Progress Report No. 5

Report 0672-01BM-5 28 May 1963

410116

AEROJET
GENERAL TIRE
GENERAL

AEROJET-GENERAL CORPORATION

SACRAMENTO, CALIFORNIA

27

4917

28 May 1963

Report 0672-01BM-5

ACOUSTICAL ANALYSIS OF FILAMENT-
WOUND POLARIS CHAMBERS

Contract NOw 62-1007c(FBM)

Bimonthly Progress Report No. 5

AEROJET-GENERAL CORPORATION
A SUBSIDIARY OF THE GENERAL TIRE & RUBBER COMPANY

ABSTRACT

This is the fifth bimonthly progress report on the program to investigate the aspects of acoustically analyzing Polaris filament-wound chambers during hydrostatic testing.

Under the contract provisions of this program, four bimonthly and one final report are required; however, because of the extension of the program completion date to 30 July 1963, this additional bimonthly progress report is required. This report, therefore, presents additional hydrostatic test results and program status.

Effort during this period was mainly concentrated on additional hydrostatic testing and reduction of data to obtain further evidence corroborating the existence of a relationship between the acceleration amplitude of the proof-pressure cycle and the chamber burst pressure. If this correlation can be firmly established, it may be possible to lower the proof pressure to a level at which a significant correlation can still be made.

TABLE OF CONTENTS

TABLE LIST

FIGURE LIST

I. OBJECTIVES

The objectives of this program are: (1) to develop sound-recording procedures so that the significance of sounds emanating from the first-stage Polaris Model A3 chambers during hydrostatic testing may be determined and (2) to determine the velocity of sound in a composite material of glass filaments and resin, the effect of the direction of filament winding on that velocity, and superimposed stress fields on that velocity.

Because of differences in the objectives, the program is divided into two phases.

A. PHASE I

The Phase I effort is directed toward the achievement of the first objective so that a noise envelope can be established that will show margins of typical behavior for a structurally sound chamber.

B. PHASE II

Work in Phase II is directed toward the achievement of the velocity-of-sound objective so that knowledge obtained from the development work can ultimately be used to establish the location of noise sources by triangulation techniques.

II. SUMMARY

This report includes a discussion of the data-presentation and data-evaluation techniques and presents the test data obtained to date from the first test objective.

II, Summary (cont.)

Results from testing in Phase I show that there is a significant relationship between the sounds emanating from a filament-wound chamber during hydrostatic testing and the structural integrity of the chamber. The measured acceleration amplitude (root mean square) during hydrostatic proof and burst testing is a function of the chamber burst pressure, and, as the data show, is inversely related to the burst pressure (Figure 1). The proof-pressure cycle acceleration amplitude may be used to establish the chamber burst pressure, and thereby define the structural integrity of the chamber.

No Phase II testing or data analysis was performed during this report period.

III. TECHNICAL DISCUSSION

A. PHASE I

1. Data Presentation

The data reported is presented in three-dimensional plots and in tabulated form. The three-dimensional surface plots of acceleration magnitude (Figures 2 through 5) show the frequency of the chamber acceleration and amplitude components as a function of hydrostatic chamber pressure. The individual frequency-amplitude plots define the magnitude surface for any amplitude level along the frequency axis. The tabulated data include average g-acceleration amplitudes to show the relative levels between similar accelerometer functions from different tests.

The three-dimensional plots are presented to show the relationship between acceleration amplitude and frequency components as a function of hydrostatic pressure. (Refer to Report 0672-01BM-4 for complete discussion of three-dimensional plots.) The presentation of three-dimensional plots for tests 645P

III, A, Phase I (cont.)

(Figures 2 and 3) and 815P (Figures 4 and 5) were included to show specifically the frequency spectrum of the proof cycle and change in the noise envelope for function G-105 (Figure 6) between the two chambers in which the only structural difference was improved doily materials on the latter chamber. The frequency spectrum shifts from a flat spectrum that is relatively independent of frequency on Test 645P to a frequency-dependent spectrum (from 126 to 2,000 cps) on Test 815P. An additional difference may be seen in the faster decrease of acceleration amplitude after 600-psig hydrostatic test pressure on Test 815P as evidenced in the 8-kc frequency sweep.

The data in Table 1 are presented to show the relative average acceleration units (g) between similar accelerometer locations on different chambers. Table 1 is a continuation of the acceleration history tabulation included in the previous progress report; at present, six chambers have been accelerometer tested to both proof and burst pressures and 10 chambers have been tested to either proof or burst pressure.

2. Data Analysis Technique

The accelerometer data obtained during hydrostatic tests are being evaluated by comparing the average acceleration amplitudes, impulse densities, and burst pressures from a series of tests. The acceleration history from a series of proof-pressure and burst-pressure cycles shows a marked relationship between acceleration amplitude and chamber burst pressure (Figure 1). The acceleration amplitude of the proof-pressure cycle from a particular chamber may be fitted to the acceleration-burst-pressure relationship to establish a burst pressure for that particular chamber.

III, A, Phase I (cont.)

3. Test Results

Representative acceleration-amplitude data from all chambers tested since the last report are shown in Table 1. Although all hydrostatically tested chambers were instrumented with multiple accelerometers (with locations as shown in Figure 6), one representative acceleration amplitude for each to three chamber sections (forward, aft, cylinder) is tabulated.

These six chambers on which both proof and burst tests were conducted are those of Tests 646P, 645P, 779P, 802P, 815P, and 814P. The acceleration-amplitude points versus burst-pressure-data points from the latter four tests, plus burst tests 843P and 801P, define a curve for both proof-pressure and burst-pressure data in Figure 1. The lines connecting data points were inserted to make the curves easier to read. The chambers in these tests were of a later design with S-994 glass. The acceleration-amplitude-data points from Tests 646P, 784P, and 645P do not fit the curve established by the six previously mentioned chambers. The Test 646P chamber had E-HTS glass, and the Test 784P chamber had E-HTS glass and a nonreversed doily; the test 645P chamber had S-994 glass but did not have improved doily materials.

A second set of average acceleration-amplitude-data points are included in Figure 1 to show the relationship that existed for the 0 to 600 psig range of the proof-pressure cycle. This relationship illustrates that chamber integrity may be established from a lower chamber-proof-pressure increment, as for example the 0 to 600 psig range evaluated.

Figure 7 is included to show the simultaneous occurrence of dynamic strain and acceleration during a hydrostatic test. The data were taken from the chamber of Test 622P, which had strain gages positioned between the wraps to

III, A, Phase I (cont.)

determine interlaminar strains. Accelerometers were located on the chamber surface at positions close to those of the strain gages. Figure 8 shows the strain gage locations relative to one function (G1) of eight accelerometers located on the chamber aft closure. Strain gage data is still being reduced and correlated with the accelerometer data to determine structural significance of the acceleration data in terms of chamber strain.

IV. FUTURE WORK

A. RECORDING OF DATA DURING HYDROSTATIC TESTS

The data recorded during hydrostatic proof and burst tests will continue to be processed and analyzed, as shown in the time schedule (Figure 9), until the relationship between the acceleration impulse and amplitude history and the burst pressure has been determined (Figure 9).

The processing of the data through the Bruel and Kjaer equipment will continue, and greater emphasis will be directed to determining the acceleration impulse versus amplitude history over the first 600 psig of the 945-psig hydrostatic proof-pressure cycle, with the objective of ultimately reducing the proof pressures.

The strain and acceleration data from Test 622P (interlaminar strain gage instrumented chamber) will be correlated to determine the structural significance of the acceleration data in terms of chamber strains.

IV, Future Work (cont.)

B. APPLICATION OF MEASUREMENTS OF VELOCITY OF SOUND

The measurements of velocity of sound already recorded and reduced will be further analyzed to determine the accuracy of measurements. The nominal velocity values obtained on the three separate chamber sections will be used to determine, by triangulation, the source of energy release during hydrostatic testing.

TABLE 1

HYDROSTATIC TEST ACCELERATION HISTORY

Test	Chamber SN	Chamber Type	Accelerometer Location	Pressure Acceleration Area, g psi	Pressure Increment, psi	Average Acceleration Amplitude, gm	Chamber Failure Area (section)
779 Proof	717072	S-994 Glass USP/Shell Resin	G105 G110	190 190	945	0.20 0.20	
802 Proof	713099	S-994 Glass CPS/Shell Resin	G105 G110 G111	614 1153 387	945 945 945	0.65 1.22 0.41	
815 Proof	715074	S-994 Glass CPS/Shell Resin	G105 G110 G111	718 1323 972	945 945 945	0.76 1.40 1.03	
814 Proof	715073	S-994 Glass USP/Shell Resin	G105 G111	765 1011	945 945	0.81 1.07	
779 Burst	717072	S-994 Glass USP/Shell Resin	G105 G110	232 232	775 (1720-945)	0.30 0.30	Center of cylinder section
801 Burst	711014	S-994 Glass USP/Shell Resin	G105	178	637 (1582-945)	0.28	Aft closure
802 Burst	713099	S-994 Glass CPS/Shell Resin	G105	197	635 (1580-945)	0.31	Aft closure
815 Burst	715074	S-994 Glass CPS/Shell Resin	G105	229	555 (1500-945)	0.41	Aft closure
814 Burst	715073	S-994 Glass USP/Shell Resin	G105	280	500 (1445-945)	0.56	Aft closure
843 Burst	713100	S-994 Glass USP/Shell Resin	G105	210	305 (1250-945)	0.69	Aft closure

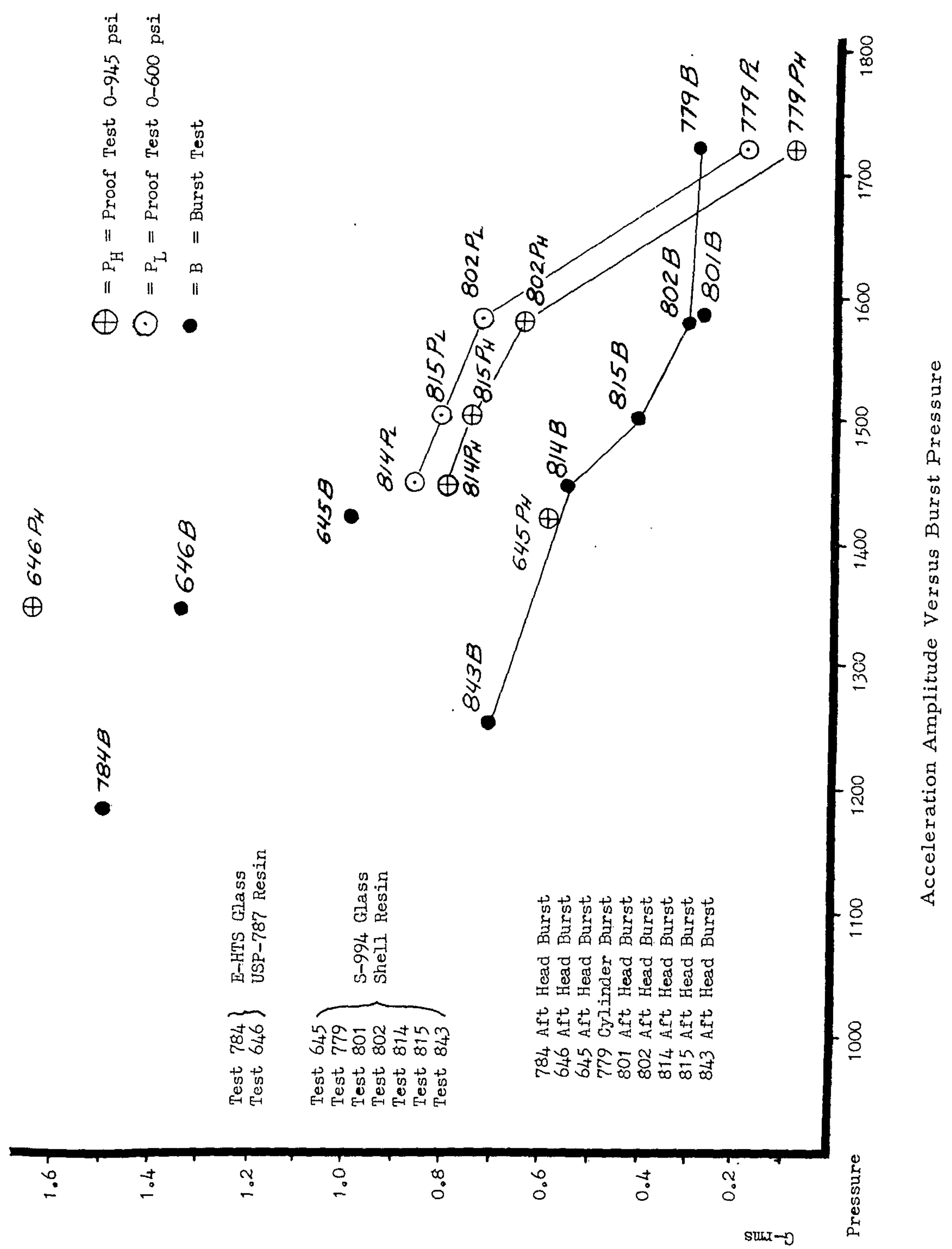
⊕ = P_H = Proof Test 0-945 psi
⊙ = P_L = Proof Test 0-600 psi
● = B = Burst Test
Test 784 } E-HTS Glass
Test 646 } USP-787 Resin
Test 645
Test 779
Test 801
Test 802
Test 814
Test 815
Test 843
S-994 Glass
Shell Resin
784 Aft Head Burst
646 Aft Head Burst
645 Aft Head Burst
779 Cylinder Burst
801 Aft Head Burst
802 Aft Head Burst
814 Aft Head Burst
815 Aft Head Burst
843 Aft Head Burst
784B
646 PH
646B
645B
645 PH
843B
814 PL
814PH
814B
815 PL
815 PH
815B
802 PL
802 PH
802B
801B
779B
779 PL
779 PH
G-rms
Pressure
Acceleration Amplitude Versus Burst Pressure
1.6
1.4
1.2
1.0
0.8
0.6
0.4
0.2
1000
1100
1200
1300
1400
1500
1600
1700
1800

Figure 1

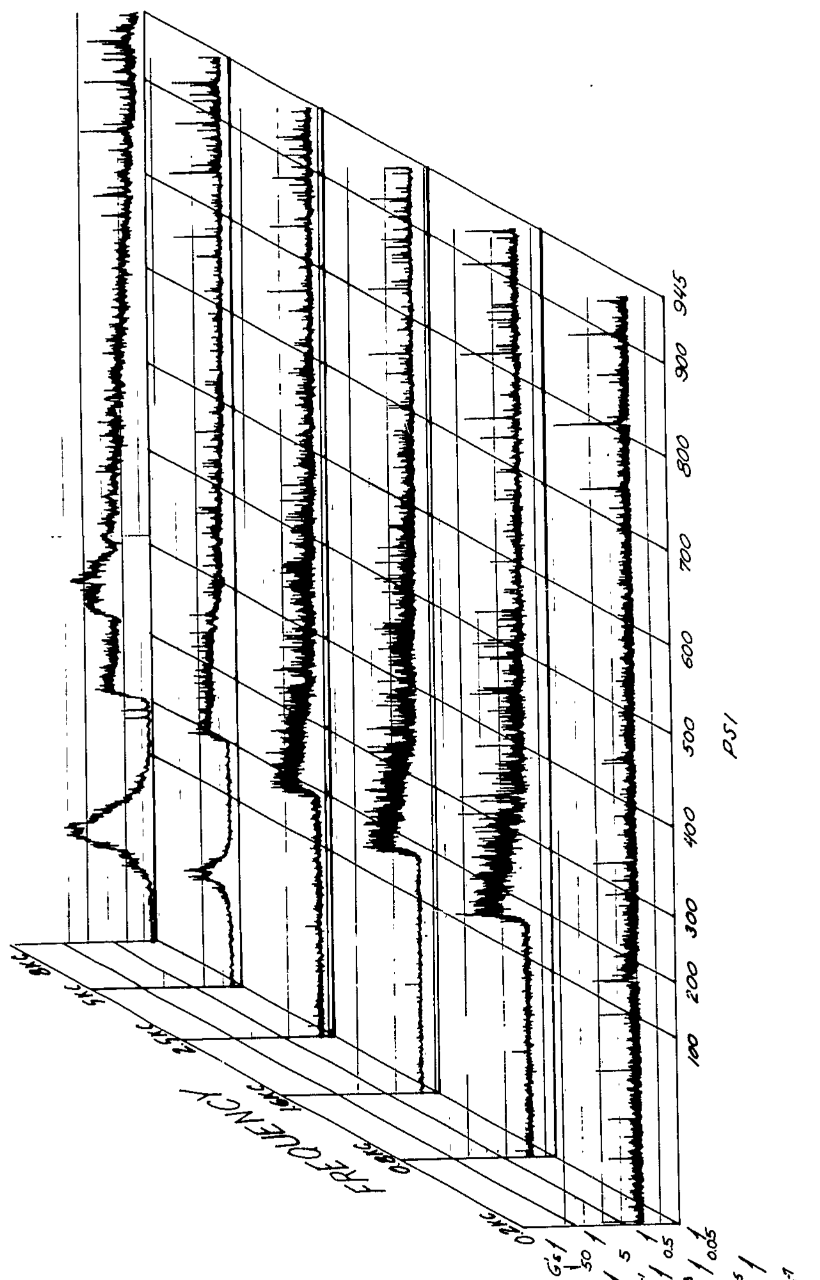

Acceleration, Magnitude Surface Plot, Proof Test 645P

Figure 2

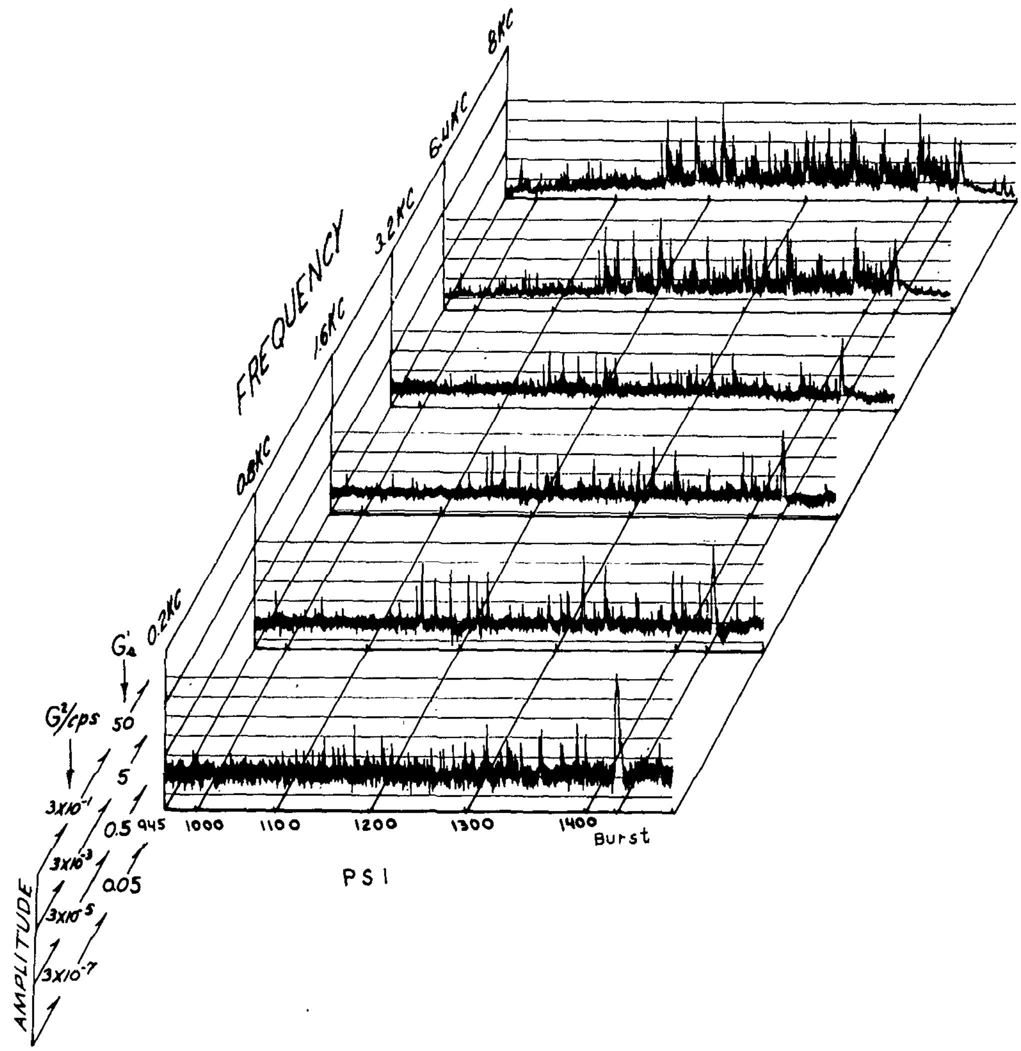

Acceleration, Magnitude Surface Plot, Bust Test 645P

Figure 3

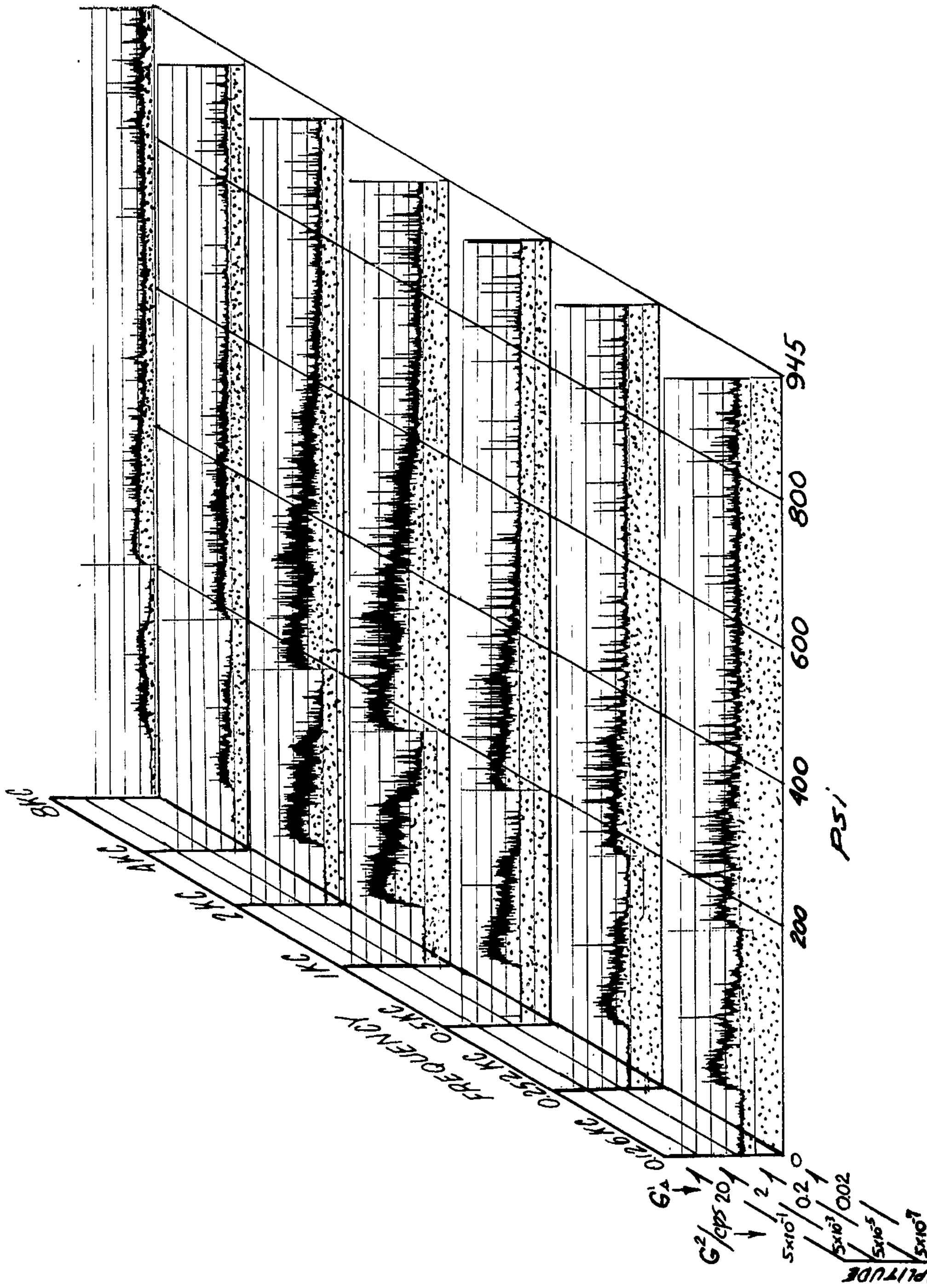

Acceleration, Magnitude Surface Plot, Proof Test 815P

Figure 4

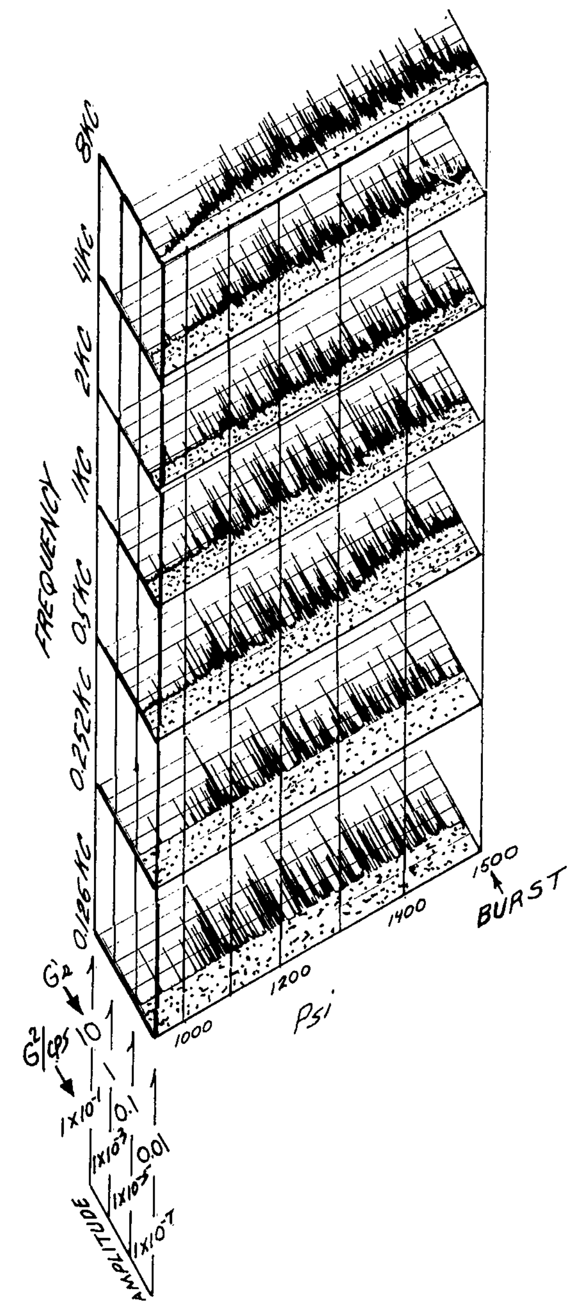

Acceleration, Magnitude Surface Plot, Burst Test 815P

Figure 5

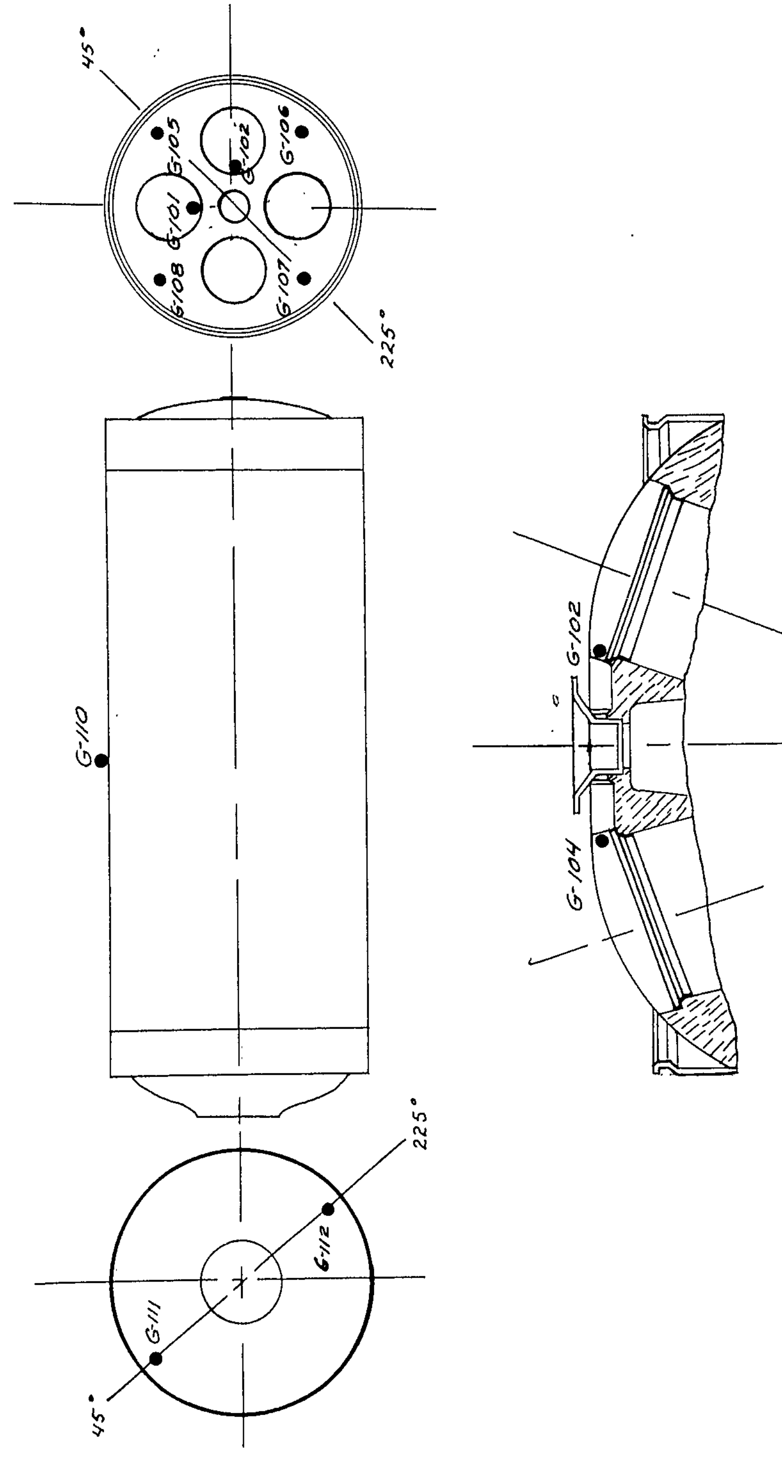

Accelerometer Locations, Hydrostatic Test

Figure 6

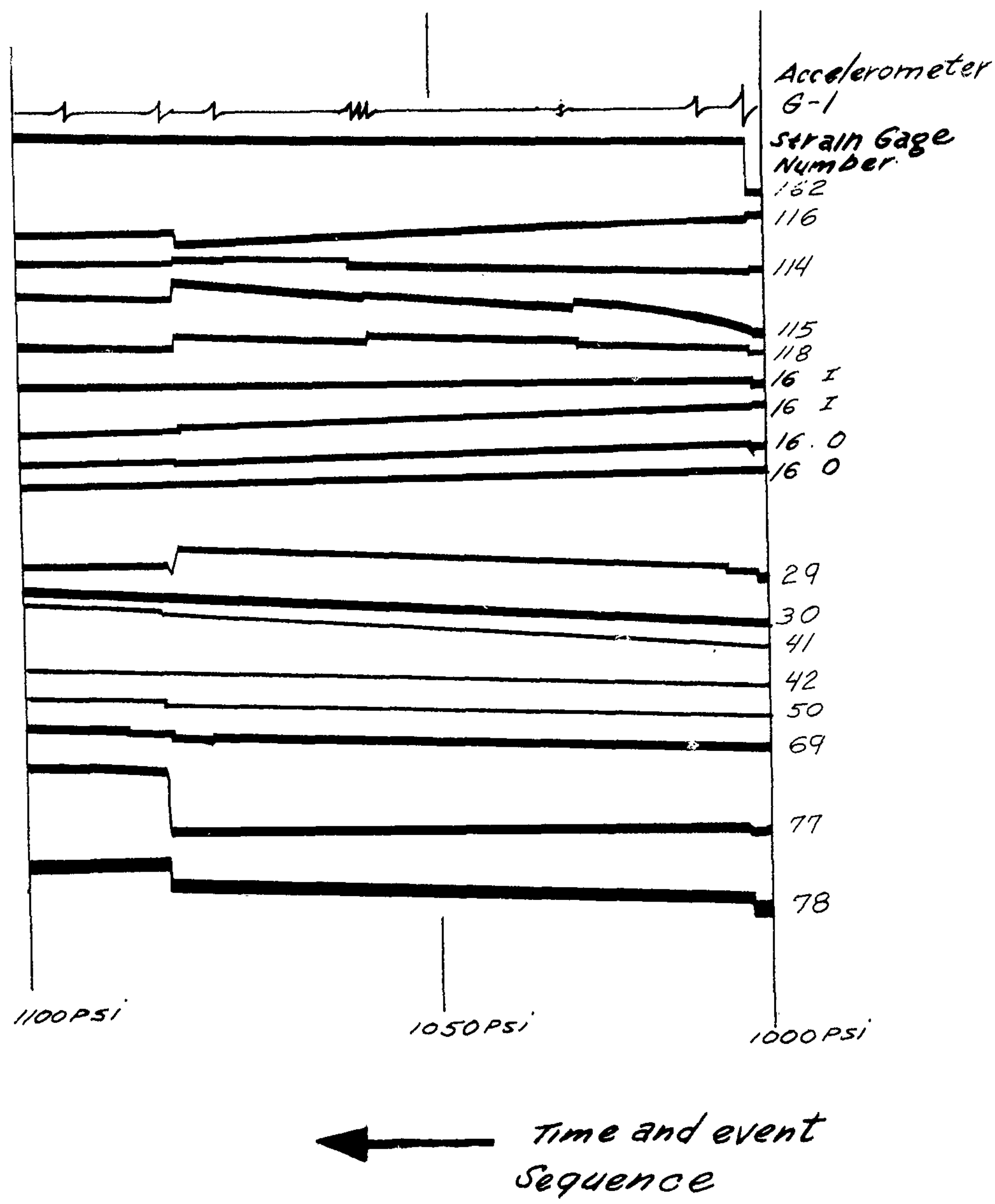

Acceleration Impulses Versus Dynamic Strain

Figure 7

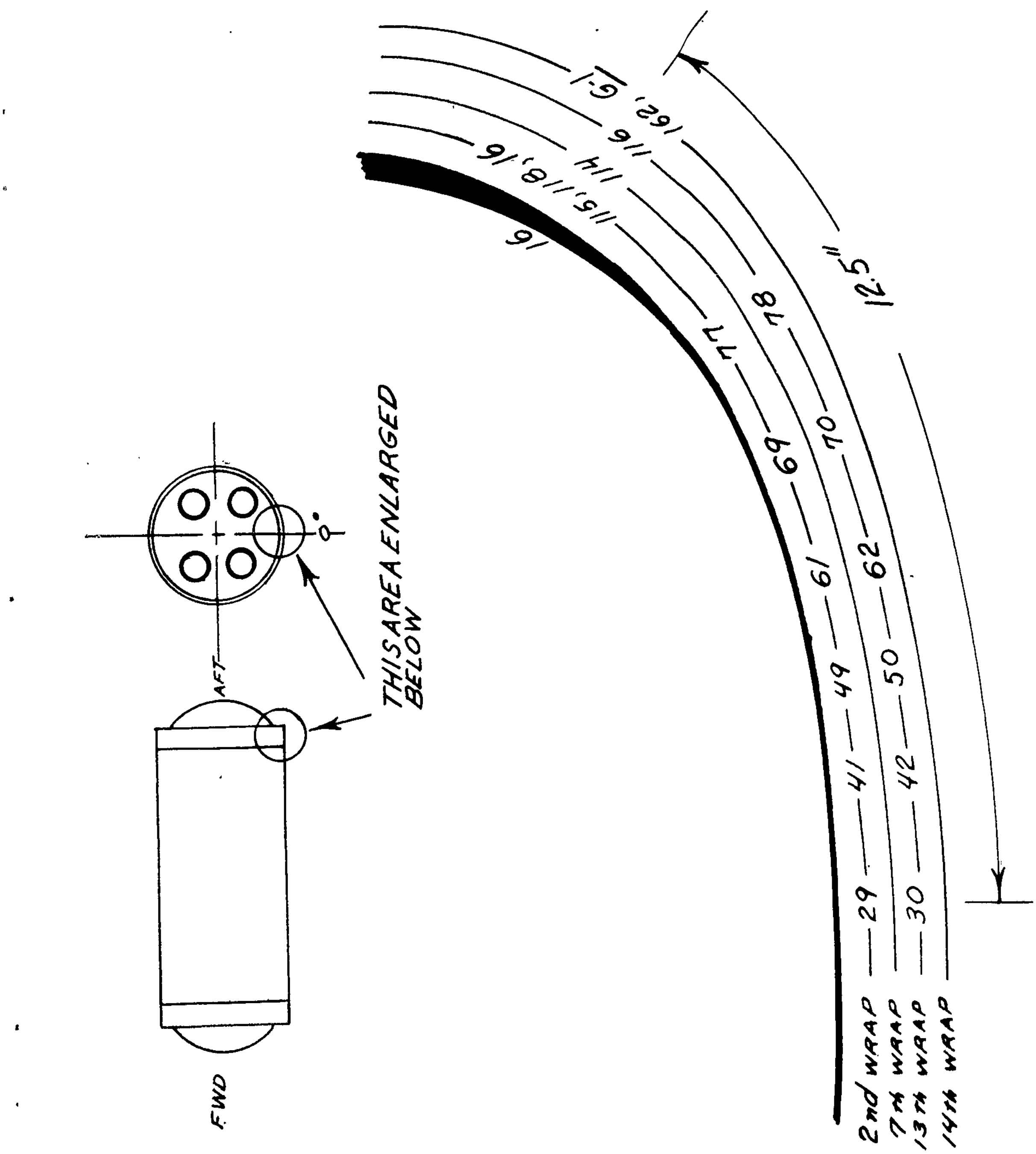

Accelerometer and Strain Gage Locations, Test 622P

Figure 8

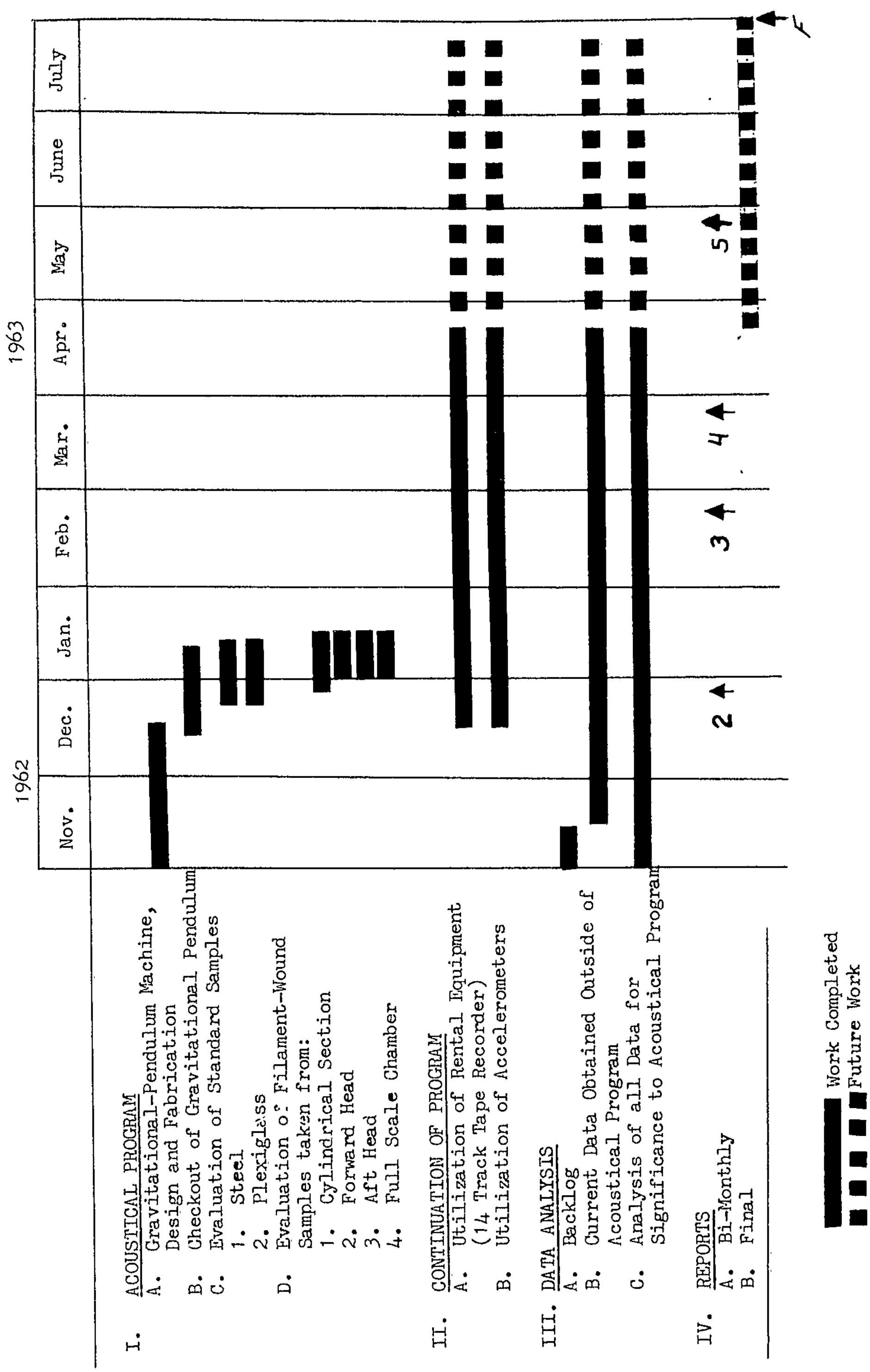

Time Schedule, Acoustics Program

Figure 9